Sci. Bull. (2015) 60(5):522–531
DOI 10.1007/s11434-015-0740-0

www.scibull.com
www.springer.com/scp

Article

Chemistry

Fe_3C-functionalized 3D nitrogen-doped carbon structures for electrochemical detection of hydrogen peroxide

Ruizhong Zhang · Wei Chen

Received: 19 November 2014 / Accepted: 25 December 2014 / Published online: 3 February 2015

Abstract Fe_3C-functionalized three-dimensional (3D) porous nitrogen-doped graphite carbon composites (Fe_3C/NG) were synthesized via a facile solution-based impregnation and pyrolysis strategy using the commercially available melamine foam and $FeCl_3$ as precursors. The structural characterizations confirmed that Fe_3C nanoparticles with an average core size about 122 nm were assembled on the surface of the carbonized melamine foam (CMF) skeletons. The electrochemical measurements demonstrated the superior electrocatalytic activity of the advanced Fe_3C/NG composite for hydrogen peroxide reduction reaction in 0.1 mol/L PBS electrolyte and the limit of detection of H_2O_2 is estimated to be 0.035 mmol/L at a signal-to-noise ratio of 3 with a wide linear detection range from 50 μmol/L to 15 mmol/L ($R^2 = 0.999$). Compared with the pure CMF, the Fe_3C/NG exhibited higher catalytic activity, more stable response, lower detection limit, higher selectivity and a wider detection range, which could be attributed to the synergic effect between the two types of active sites from the iron carbide species and the nitrogen-doped graphite carbon. Meanwhile, the large surface area, high conductivity and the improved mass transport from the 3D porous material can also promote the electrochemical sensing performance. Moreover, the Fe_3C/NG-based electrochemical sensor showed high anti-interference ability and stability for H_2O_2 detection. Thus, the novel and low-cost Fe_3C/NG composite may be a promising alternative to noble metals and offer potential applications in various types of electrochemical sensors, bioelectronic devices and catalysts.

Keywords Melamine foam · Nitrogen-doped carbon · Fe_3C nanoparticles · Hydrogen peroxide · Electrochemical sensor · Biosensor

1 Introduction

Hydrogen peroxide (H_2O_2) has been found to take part in a wide range of enzymatic reactions and plays important roles in the fields of food [1], textile industry [2], chemical synthesis [3], pharmaceutical analyses [4], environmental protection [5], etc. Meanwhile, H_2O_2 reduction is of widespread interest to bioanalytical science because it often serves as an electroactive reporter molecule in the indirect detection of biomolecules, e.g., glucose [6, 7]. Therefore, different materials and methods have been developed for the high-performance detection of H_2O_2. Up to now, many detection techniques have been well developed, such as titrimetry [8, 9], photometry [10], chemiluminescence [11] and electrochemistry [12–14]. Of them, electrochemical technique has been recognized as one of the best methods for H_2O_2 detection for its intrinsic simplicity, high sensitivity and good selectivity. Most of the electrochemical sensors with the participation of the enzyme can speed up the electron transfer between the electrodes and H_2O_2 [15, 16]. However, the application of

R. Zhang · W. Chen (✉)
State Key Laboratory of Electroanalytical Chemistry, Changchun Institute of Applied Chemistry, Chinese Academy of Sciences, Changchun 130022, China
e-mail: weichen@ciac.ac.cn

R. Zhang
University of Chinese Academy of Sciences, Beijing 100049, China

enzyme-based sensors is limited because the enzyme is expensive and easy to denature. Such problem was later solved by using nanostructures such as carbon nanotubes (CNTs), noble metal nanoparticles, as catalysts to catalyze the oxidation or reduction of H_2O_2. Among the developed nanostructures, noble metal materials, such as Pt, Pd, Au and Ag, are usually used as catalysts for H_2O_2 detection with electrochemical method. To decrease the cost of the sensors fabricated from noble metals, it is necessary to develop highly sensitive, reliable and low-cost biosensors with excellent electrocatalytic activity for the oxidation or reduction of H_2O_2. Accordingly, much attention has been devoted to rational design of non-precious metals or metal-free catalysts with unique architectures to dramatically enhance the catalytic activity. Recently, Guo's group [17] synthesized the composite of Cu-based metal–organic frameworks loaded in macroporous carbon, Tian et al. [18] prepared the ultrathin carbon nitride nanosheets, and our group [19] synthesized the graphene-wrapped Cu_2O nanocubes. All the prepared non-precious metal or metal-free nanostructures can serve as efficient electrocatalysts toward the reduction of hydrogen peroxide.

Porous carbon materials have many unique properties, such as high surface area, thermal and chemical stability, highly electrical conductivity and hydrophobic surface properties, which render them suitable for potential application as adsorbents, energy storage materials and catalyst supports [20–23]. However, because their surfaces are chemically inert, carbon materials themselves show low catalytic activity. In recent years, it was found that the incorporation of nitrogen heteroatoms into carbon frameworks, such as mesoporous carbons and novel nanostructured carbons with one-, two- or three-dimensional (3D) structures, including graphite nanofibers (GNFs), CNTs and graphene, through post hoc and/or in situ doping can alter the properties including electrical conductivity, basicity and oxidation stability. On the other hand, heteroatom dopants can also change the surface chemical states of carbon and thus improve the catalytic activities of carbon materials. Notably, since Jasinski's [24] pioneering work, which showed that cobalt phthalocyanines are electrocatalytically active for oxygen reduction reaction (ORR), non-noble metal catalysts based on transition metals and nitrogen functionalities have been drawing more and more attention and various kinds of nitrogen-containing materials have been developed [25, 26]. Although the exact reaction mechanism of these non-noble catalysts remains controversial, the enhanced activity is likely attributed to the fact that the introduction of N atom leads to the formation of nitrogen macrocycle during carbonization. These nitrogen-doped carbon materials have been extensively studied as cathode catalysts in proton exchange membrane fuel cells (PEMFCs) because of their remarkable ORR catalytic activities and high durability and low cost. Recently, nitrogen-rich materials (aniline, cyanamide, dicyandiamide and urea, etc.) were used as nitrogen and/or carbon sources in the preparation of porous carbon-based non-precious metal or metal-free catalysts [27–30]. For example, Parvez [27] used cyanamide as a nitrogen source and graphene as a precursor to prepare nitrogen-doped graphene and its iron-based composites through incorporation of iron chloride. Xia' group [28] prepared the N-doped graphene by thermal annealing graphite oxide using melamine as nitrogen source. In another work, Zhong et al. [29] synthesized nitrogen-doped carbon xerogel catalysts from melamine formaldehyde resin. All these N-doped carbon materials demonstrated excellent electrocatalytic performance for ORR. Importantly, as the second procedure of ORR, the catalytic reduction of hydrogen peroxide is also an important process for developing electrochemical detection of H_2O_2. However, to our best knowledge, the commercial melamine foam is seldom used as precursor to directly synthesize 3D nitrogen-doped porous carbon as catalysts for electrochemical sensing of hydrogen peroxide.

Herein, we report the facile synthesis of Fe_3C-functionalized nitrogen-doped graphitic carbon composite (Fe_3C/NG) through the pyrolysis of low-cost melamine foam and iron salts ($FeCl_3$) by controlling the pyrolysis temperature. The electrochemical measurements demonstrated that the as-prepared 3D Fe_3C/NG composite exhibits superior electrocatalytic activity for hydrogen peroxide reduction in 0.1 mol/L phosphate-buffered saline (PBS) electrolyte. With the Fe_3C/NG composite as sensing material, the limit of detection (LOD) of H_2O_2 was estimated to be 0.035 mmol/L at a signal-to-noise ratio of 3 with a wide linear detection range from 50 μmol/L to 15 mmol/L ($R^2 = 0.999$). The present study indicates that the as-prepared 3D Fe_3C/NG composites have potential application in electrochemically detecting H_2O_2 as high-performance electrode materials.

2 Experimental

2.1 Chemicals

L-ascorbic acid (AA), H_2O_2 (A.R. grade, ≥30 %), disodium hydrogen phosphate dodecahydrate ($Na_2HPO_4{\cdot}12H_2O$, A.R. grade, ≥99.0 %), sodium dihydrogen phosphate dihydrate ($NaH_2PO_4{\cdot}2H_2O$, A.R. grade, ≥99.0 %) and ethanol (absolute ethanol, A.R. grade, ≥99.7 %) were purchased from Beijing Chemical Works. Dopamine (DA) and uric acid (UA) were obtained from Aladdin and Sigma, respectively. Ferric chloride ($FeCl_3{\cdot}6H_2O$, A.R. grade, ≥99.0 %) was obtained from

Tianjin Chemical Reagent of East China, and melamine foam was supplied by Puyang Green Universh Chemical Co., Ltd. All aqueous solutions were prepared with ultrapure water (18.25 MΩ cm). Ultrapure N_2 gas (≥99.999 %) was supplied by the Changchun Juyang Gas Limited Liability Company.

2.2 Synthesis of Fe_3C/NG catalyst

In a typical experiment, 150 mL 0.006 mol/L $FeCl_3$ solution was first prepared with absolute ethanol. Then, several slices (0.5034 g) of commercially available melamine foam were soaked with the pre-prepared ferric chloride suspension in a water bath at 60 °C for 24 h. The melamine foam impregnated with $FeCl_3$ ethanol solution was dried at 70 °C for 12 h until it thoroughly dried and then pyrolyzed under Ar atmosphere at 1,000 °C for 1 h (with a heating rate of 3 °C/min). Finally, the carbonized catalysts were leached with 2 mol/L H_2SO_4 at 60 °C for 3 h to remove unstable species and excess metallic iron and iron oxides. The resulting samples were separated by centrifugation and washed with ultrapure water and absolute alcohol for several times. Finally, the product was dried in a drying oven and abbreviated as Fe_3C/NG. For comparison, carbonized melamine foam (CMF) was also prepared in a similar way without the addition of iron salts.

2.3 Characterization

The morphologies of the as-prepared materials were characterized with a XL30 ESEMFEG scanning electron microscope (SEM) operating at an accelerating voltage of 20 kV. Elemental analyses of the materials were carried out using techniques of energy dispersive X-ray spectroscopy (EDS), equipped in the FE-SEM. Powder X-ray diffraction (XRD) was performed on a D8 Advance using Cu Kα radiation with a Ni filter ($\lambda = 0.154059$ nm at 30 kV and 15 mA) to examine the crystallinity of the products. X-ray photoelectron spectroscopy (XPS) measurements were performed by using a VG Thermo ESCALAB 250 spectrometer operated at 120 W. The binding energy was calibrated against the carbon 1s line. The compositions of the products were determined by inductively coupled plasma atomic emission spectrometer (ICP-AES, X Series2).

2.4 Electrochemical measurements

Before each experiment, a glassy carbon (GC) electrode (3.0 mm in diameter) was first polished with alumina slurries (Al_2O_3, 0.05 μm) on a polishing cloth to obtain a mirror finish, followed by sonication in 0.1 mol/L HNO_3, 0.1 mol/L H_2SO_4 and pure water for 10 min, successively. To prepare a catalyst-coated working electrode, 1 mg/mL catalyst suspension were prepared by ultrasonically blending 2 mg of the catalyst and 19.8 μL of 5 wt% Nafion suspension in alcohol (Solution Technology, Inc.) for 30 min, in 1.98 mL solution containing isopropanol and deionized water (4:1 by volume). And then 5 μL of the 1 mg/mL suspension was drop-coated on the polished electrode surface by a microliter syringe, followed by drying at room temperature. The loading of the catalyst on the GC electrode is 5 μg. All electrochemical experiments were carried out at room temperature.

Cyclic voltammetry (CV) and amperomeric current–time measurements were carried out with a CHI660D electrochemical workstation. The electrodes prepared above were used as the working electrodes. An Ag/AgCl (in saturated KCl aq.) combination isolated in a double junction chamber and a Pt wire were used as the reference and counter electrodes,respectively. All electrode potentials in the present study were referred to this Ag/AgCl reference. The working electrodes were first activated with CV (−1.2 to 0 V at 0.2 V/s) in N_2-saturated 0.1 mol/L PBS solution (pH 7.4) until a steady CV was obtained. To measure hydrogen peroxide reduction reaction, different concentrations of hydrogen peroxide stock solution were added into the N_2-purged 0.1 mol/L PBS solution, and the CVs were recorded in a potential window between −1.2 and 0.0 V at a scan rate of 50 mV/s. The amperometric current–time (*i–t*) curves were measured at −0.6 V for 3,500 s in 0.1 mol/L PBS saturated with N_2 gas. Amperometry was used to monitor the current change during successive injections at 100 s intervals that resulted in an incremental 0.5 mmol/L H_2O_2 concentration.

3 Results and discussion

3.1 Synthesis and characterization of Fe_3C/NG composites

In the present study, a facile impregnation and pyrolysis strategy was developed to synthesize precious metal-free catalyst. The morphologies of the as-synthesized products were first characterized by SEM. Figure 1a shows the representative SEM image of CMF after pyrolysis at 1,000 °C for 1 h, demonstrating an open-cell network structure from a cross-sectional view. This unique architecture can offer high specific surface area and large amount of pore volume for supporting nanoparticles. From the SEM images at different magnifications indicated in Fig. 1b, c, iron-contained nanoparticles are formed on the surfaces of the carbon foam skeletons after the commercially available melamine foam impregnated with ferric chloride were thermolysized at high temperature.

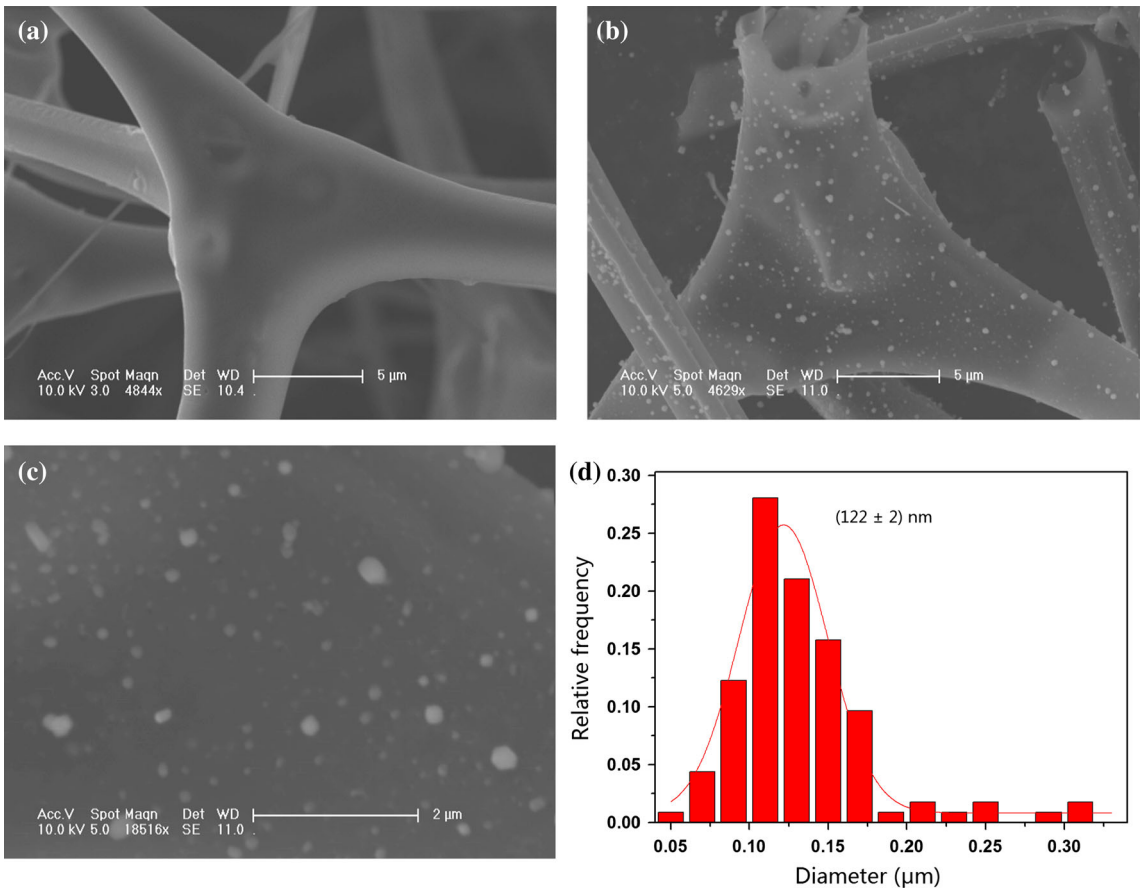

Fig. 1 (Color online) SEM micrographs of the as-prepared samples: CMF (**a**) and Fe_3C/NG samples at different magnifications (**b**, **c**). **d** The corresponding size distribution histogram of the Fe_3C nanoparticles

Moreover, 150 nanoparticles were randomly selected to measure the particle size. From the diameter distribution histogram shown in Fig. 1d, the as-prepared nanoparticles have an average core diameter of (122 ± 2) nm. Based on above structural characterization, Fe-based nanoparticles have been successfully synthesized and assembled on the surfaces of the CMF.

The crystalline phase and the corresponding elements of the as-prepared product were characterized by XRD, EDS and XPS. The XRD pattern of the Fe_3C/NG composite is shown in Fig. 2a. The clear diffraction peaks with 2θ at 37.6°, 37.8°, 42.9°, 43.8°, 44.6°, 45.0°, 45.9°, 48.6° and 49.1° could be indexed to the (121), (210), (211), (102), (220), (031), (112), (131) and (221) planes of Fe_3C according to the diffraction data of bulk Fe_3C (JCPDS No. 65-2413). The formation of Fe_3C nanoparticles could be due to the easy bonding and interaction of iron precursor with amorphous nitrogen-doped graphite carbon by coordination with nitrogen and carbon within the micropores, resulting in the further production of Fe_3C nanoparticals during the pyrolysis process. Note that the peak with 2θ at around 25° could be ascribed to the (002) plane of graphite carbon. Such XRD pattern has also been observed in other hybrid materials [23]. The XRD analysis indicates that metal carbide (Fe_3C) and graphite carbon co-exist in the Fe_3C/NG composites. The content of the Fe_3C/NG composites was further analyzed by EDS and ICP-AES. From the EDS measurement shown in Fig. 2b, elements of Fe, N, O, S and C are present in the composites, and the contents were calculated to be 1.74 at.%, 5.3 at.% and 85.21 at.% for Fe, N and C, respectively, which agrees well with the ICP-AES result (1.956 at.% for Fe). The composition and oxidation states of the as-prepared Fe_3C/NG composite were investigated by XPS measurements. The survey XPS spectra of the as-prepared CMF and Fe_3C/NG composite are shown in Fig. 2c. Both spectra show clearly the presence of C, N and O. However, compared with the spectrum of CMF, a peak ranging from 710 to 740 eV indexed to Fe 2p [25] can be observed in the spectrum of Fe_3C/NG composite, although the peak is weak owing to the low iron content (1.74 at.%) from the EDS measurement. From the C 1s spectrum of the Fe_3C/NG shown in Fig. 2d, the three fitted peaks can be assigned to the binding energies of carbon in C=C/C–C, C–N and C=N, respectively. These

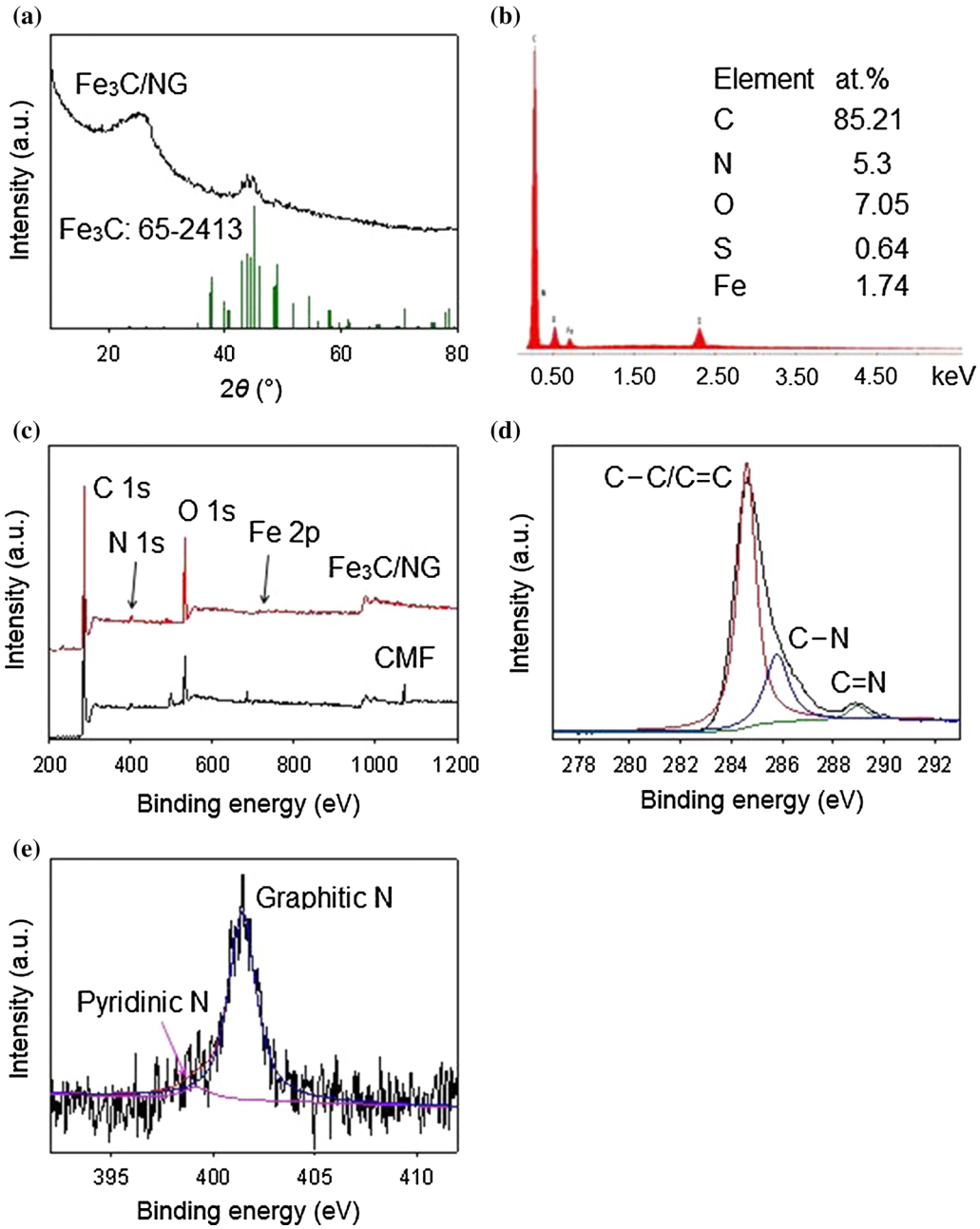

Fig. 2 (Color online) **a** XRD pattern of the as-prepared Fe_3C/NG composite. For comparison, bulk Fe_3C phase from the JCPDS (65-2413) is also presented. **b** EDS analysis of the Fe_3C/NG composite. **c** Survey XPS spectra of the as-prepared CMF and Fe_3C/NG composite. **d** High-resolution C 1s XPS spectrum of the Fe_3C/NG composite. **e** High-resolution N 1s XPS spectrum of the Fe_3C/NG composite

XPS results suggest the complete conversion of melamine foam into graphite carbon and the incorporation of N atoms into the composites during the pyrolysis process, resulting in the nitrogen-doped graphite carbon. Such results agree well with the previously reported results [28]. The high-resolution N 1s spectrum (Fig. 2e) further indicates the N-doping in graphitic carbon for the Fe_3C/NG composites. The deconvoluted two peaks at 399.19 and 401.44 eV correspond to pyridinic [30, 31] and graphitic [31] nitrogen species. Moreover, for the two nitrogen species, the peak intensity of the graphitic nitrogen, which is believed to be mainly responsible for the high oxygen reduction reaction activity, is significantly higher than that of the pyridinic nitrogen.

3.2 Electrocatalytic activity of the Fe_3C/NG composite for H_2O_2 reduction and the application in electrochemical detection of H_2O_2

The electrocatalytic activity of Fe_3C/NG composite for H_2O_2 reduction was first studied by electrochemical CV. For comparison, CMF prepared by the same synthetic process was also examined. Before the electrochemical measurements, all the GC-supported catalysts were first activated with CV (−1.2 to 0 V at 0.2 V/s) in N_2-saturated 0.1 mol/L PBS solution (pH 7.4) until a steady CV was obtained. Figure 3a, b shows the CVs of Fe_3C/NG composite and CMF in N_2-saturated 0.1 mol/L PBS (pH 7.4) solution with the absence and presence of 7.5 mmol/L H_2O_2. It can be seen that the CV of the Fe_3C/NG composite shows large double-layer charging current in 0.1 mol/L PBS. Upon the addition of 7.5 mmol/L H_2O_2, enhanced reduction current can be observed, indicating the high electrocatalytic activity for H_2O_2 reduction. In sharp contrast, under the same experimental condition, only weak

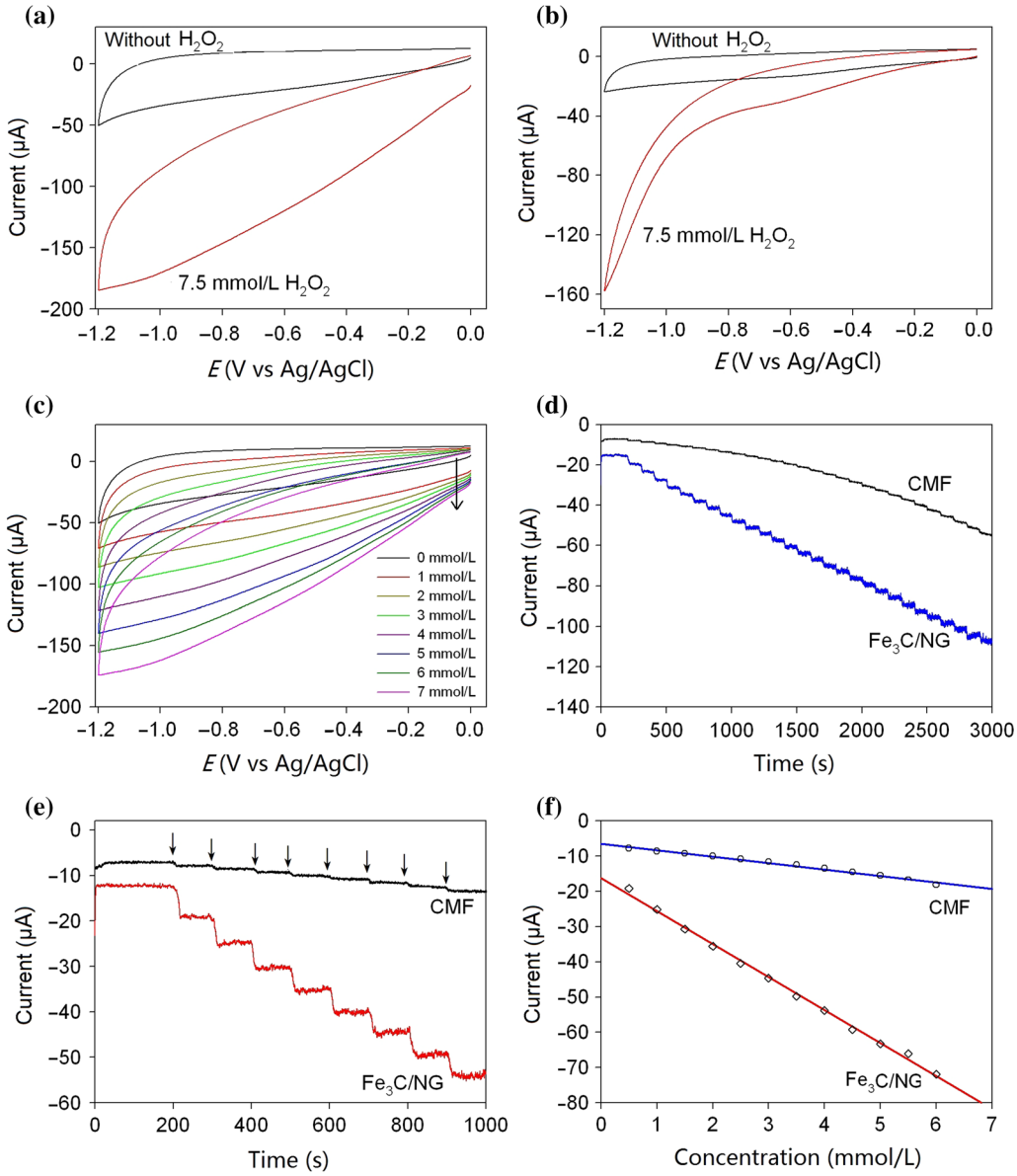

Fig. 3 (Color online) CVs of glassy carbon electrodes modified with Fe_3C/NG (**a**) and CMF (**b**) in N_2-saturated 0.1 mol/L PBS (pH 7.4) without and with the presence of 7.5 mmol/L H_2O_2. Potential scan rate 50 mV/s. **c** CVs of glassy carbon electrode modified with Fe_3C/NG composites in N_2-saturated 0.1 mol/L PBS with different concentrations of H_2O_2. Potential scan rate 50 mV/s. **d**, **e** Representative amperometric *i*–*t* curves of glassy carbon electrodes modified with Fe_3C/NG and CMF at different magnifications during H_2O_2 injections (black arrows, 10 μL each) into the stirred 0.1 mol/L PBS solution. **f** The corresponding calibration curves for the H_2O_2 detections on the Fe_3C/NG and CMF

reduction current was produced on CMF-modified GC electrode with the addition of 7.5 mmol/L H_2O_2 into the electrolyte (Fig. 3b), suggesting the low electrocatalytic activity of CMF for H_2O_2 reduction. For example, at −0.6 V (vs. Ag/AgCl), the reduction current obtained from the Fe_3C/NG composite (119.8 μA) is around 4.1 times greater than that of CMF (28.91 μA). This CV comparison shows that the deposition of Fe_3C nanoparticles on 3D porous nitrogen-doped graphite carbon can significantly enhance the catalytic activity for the electro-reduction of hydrogen peroxide. Meanwhile, the electrochemical response of the Fe_3C/NG composite to different concentrations of H_2O_2 was also studied. As shown in Fig. 3c, the current density of H_2O_2 reduction increases with the increasing of H_2O_2 concentration, demonstrating an outstanding sensitivity to the concentration change of hydrogen peroxide. Therefore, the prepared non-precious metal composite catalyst (Fe_3C/NG) can be used as 3D electrochemical sensing material for the detection of hydrogen peroxide. The high electrochemical sensing performance of the Fe_3C/NG for H_2O_2 detection could be ascribed to the unique nanostructure of Fe_3C/NG. The present nitrogen-doped carbon composite (Fe_3C/NG) can not only provide high conductivity and large surface area from the 3D and porous carbon skeleton, but also enhance the mass transport in the electrochemical detection due to the porous structure. Meanwhile, the exteriorly and interiorly exposed Fe_3C catalytic species in the porous structure can provide plenty of electrochemically active sites to promote the H_2O_2 reduction reaction.

The electrochemical sensing performances of the Fe_3C/NG and CMF for H_2O_2 detection were then studied. In the experiments, amperometry was performed at −0.6 V (vs. Ag/AgCl) in stirred 0.1 mol/L PBS (pH 7.4) during successive injections at 100 s intervals that resulted in an incremental 0.5 mmol/L H_2O_2 concentration. The typical amperometric *i*–*t* curves for Fe_3C/NG composite and CMF catalyst are shown in Fig. 3d. The two *i*–*t* curves illustrate a notable difference in current response. First, the Fe_3C/NG composite exhibits a significantly greater current response toward H_2O_2 compared with CMF. Second, a linear relationship between current and concentration of H_2O_2 can be observed at the Fe_3C/NG in a wider concentration range compared with the CMF. Furthermore, consistent and well-defined amperometric step response can be observed for nearly 30 consecutive H_2O_2 injections (15 mmol/L H_2O_2) and the electrode achieved 95 % of the steady-state-current within 5 s at the Fe_3C/NG composite system, while the CMF system displayed a much smaller and less-defined step response. All these results can be further observed from the higher-magnified *i*–*t* curves shown in Fig. 3e. Clearly, H_2O_2 injections (black arrows) at the CMF-modified GC electrode result in a very small amperometric response whereas the same injections at the Fe_3C/NG composite result in a significantly enhanced current signal. For example, the first injection (i.e., the first step), resulting in a 0.5 mmol/L H_2O_2 bulk solution, yields a cathodic current (∼19.22 μA) from the H_2O_2 reduction which is 2.45 times greater than the same injection at a CMF-modified electrode (∼7.84 μA). Figure 3f illustrates the dependence of current on the added concentration of H_2O_2 on the two electrodes (calibration curves). It can be seen that at CMF-modified electrode, there is only a little increase in reduction current with increasing the concentration of H_2O_2, exhibiting a low sensitivity (small slope) of only 1.73 (μA L)/mmol. However, at the Fe_3C/NG composite, obvious reduction current change can be observed with H_2O_2 injections (large slope). The sensitivity of 9.44 (μA L)/mmol obtained from the Fe_3C/NG composite is more than 5.46 times greater than that of the CMF. Moreover, detection of H_2O_2 can be achieved at the Fe_3C/NG composite over a much wider range of concentrations. For the Fe_3C/NG composite, the minimum detectable concentration of H_2O_2 is estimated to be 0.035 mmol/L at a signal-to-noise ratio of 3 with a wide linear detection range from 50 μmol/L to 15 mmol/L ($R^2 = 0.999$). It should be pointed out that the obtained linear detection range from the present 3D Fe_3C/NG nanostructure is much wider than the 1.76–139 μmol/L for NCNT [32], 0.5–150 μmol/L for sheet-like Fe_3O_4–PDDA [33], 10 μmol/L to 3.03 mmol/L for MnO_2/Nafion [34], 1 μmol/L to 3.03 mmol/L for Cu_2S/OMCs/Nafion [35] and several other recently reported sensors [36, 37]. However, the detection limit of 0.39 mmol/L ($R^2 = 0.992$) was obtained from the CMF-based H_2O_2 sensor, which is 11 times higher than that of the Fe_3C/NG composite. Moreover, a much narrower linear detection range from 0.5 to 5.5 mmol/L was achieved from the CMF. All these results indicate that the Fe_3C/NG composite materials have high catalytic activity for H_2O_2 reduction and the 3D composite structure can be used for electrochemical sensing of hydrogen peroxide with an outstanding sensitivity. On the other hand, although the CMF showed catalytic activity, to some degree, for H_2O_2 reduction, it exhibited much lower current and sensitivity, and narrower limit detection range compared with the Fe_3C/NG composite. Therefore, the incorporation of Fe_3C species into CMF skeletons via the co-pyrolysis of $FeCl_3$ and melamine foam precursors can significantly enhance the catalytic activity for hydrogen peroxide reduction and thus the sensing performance for electrochemical detection of hydrogen peroxide. The improved catalytic activity of Fe_3C/NG composite may be ascribed to the two types of catalytically active sites: the iron carbide supported on the melamine skeleton and the nitrogen-doped graphite carbon.

3.3 Selectivity and stability of Fe_3C/NG composite electrocatalyst

As it is well known that some co-existing electroactive species in nature may affect the sensing response for hydrogen peroxide. Here, the sensing interference caused by common species, including AA, UA and DA was investigated. In the interference experiments, the concentrations of H_2O_2 and other interfering species are 1 and 0.1 mmol/L, respectively, based on their physiological levels [38, 39]. Figure 4a shows the amperometric responses of the Fe_3C/NG composite- and CMF-modified GC electrodes at −0.6 V to 1 mmol/L H_2O_2, and 0.1 mmol/L of different interfering species in a stirring 0.1 mol/L PBS solution (pH 7.4). It can be seen that at the CMF-modified GC electrode, there is only a weak current change upon the addition of 1 mmol/L H_2O_2. Moreover, a sharp decrease in reduction current upon the addition of DA is observed for the CMF-modified electrode (Fig. 4a inset). In contrast, the amperometric responses from Fe_3C/NG composite-modified electrode show negligible current changes with addition of the interfering species compared with current from H_2O_2, indicating much better tolerance and higher selectivity than the CMF electrocatalyst. The results also indicate that the Fe_3C/NG composite catalyst has higher tolerance to AA, UA and DA compared with some noble metal-based biosensors [40–42].

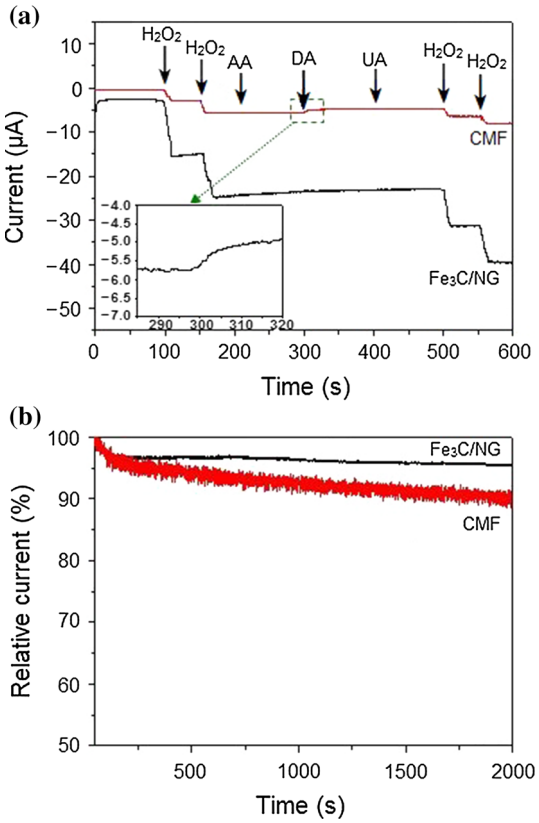

Fig. 4 (Color online) **a** Amperometric responses of the Fe_3C/NG composite- and CMF-modified GC electrodes at −0.6 V to 1 mmol/L H_2O_2, and 0.1 mmol/L of different interfering species of AA, DA and UA, in a stirring 0.1 mol/L PBS solution (pH 7.4). Inset shows the magnified current signal upon the addition of DA at the CMF. **b** Current–time chronoamperometric responses of the Fe_3C/NG composite- and CMF-modified GC electrode at −0.6 V in N_2-saturated 0.1 mol/L PBS (pH 7.4) under stirring

In addition to activity, stability of a catalyst is also one of the critical issues for its application in electrochemical sensors. To investigate the stabilities of the Fe_3C/NG composite and CMF, the current changes were recorded by holding the two electrodes at −0.6 V for 2,000 s in a 0.1 mol/L PBS solution (pH 7.4) saturated with nitrogen under stirring. The corresponding chronoamperometric responses of the Fe_3C/NG composite and CMF are shown in Fig. 4b. As can be seen, 95.4 % current from the Fe_3C/NG composite was preserved after the operation, whereas the relative current decreased to 90.8 % at the CMF catalyst. This result indicates the stability of Fe_3C/NG composite is much higher than that of the CMF. The above electrochemical measurements indicate that the Fe_3C/NG composite exhibits high electrocatalytic activity and stability for hydrogen peroxide reduction, and thus, they have promising application in electrochemical sensor for sensitive and selective detection of hydrogen peroxide. Moreover, such 3D nanostructure demonstrates highly competitive performance but much lower cost compared with the sensors based on noble metal catalysts.

4 Conclusion

In this study, a facile impregnation and pyrolysis strategy was developed to synthesize well-defined 3D porous Fe_3C/NG composite by using the commercially available melamine foam and $FeCl_3$ as precursors. The structural characterizations showed that the Fe_3C nanoparticles with an average core size about 122 nm were dispersed on the surface of CMF skeletons. The electrocatalytic activity of the Fe_3C/NG composite and CMF toward the hydrogen peroxide reduction reaction were examined by cyclic voltammetry, chronoamperometric in 0.1 mol/L PBS electrolyte. Compared with the CMF, the Fe_3C/NG composite exhibited superior electrocatalytic activity for H_2O_2 reduction, which could be attributed to a significant synergic effect from the two types of active sites between the iron carbide-functionalized melamine foam skeleton and the nitrogen-doped graphite carbon. Owing to the high catalytic activity, the electrochemical sensor fabricated from the Fe_3C/NG composite exhibited excellent sensing performance for the detection of hydrogen peroxide with rapid response, low detection limit, high selectivity and a

wide detection range. This study shows that such novel and low-cost 3D non-precious metal composite material may be a promising alternative for noble metal-based catalysts and offer potential applications in various types of biosensors, bioelectronic devices and catalysts.

Acknowledgments This work was supported by the National Natural Science Foundation of China (21275136) and the Natural Science Foundation of Jilin Province (201215090).

Conflict of interest The authors declare that they have no conflict of interest.

References

1. Charisiadis P, Tsiafoulis CG, Exarchou V et al (2012) Rapid and direct low micromolar nmr method for the simultaneous detection of hydrogen peroxide and phenolics in plant extracts. J Agric Food Chem 60:4508–4513
2. Tanaka A, Iijima M, Kikuchi Y et al (1990) Determination of hydrogen peroxide in fish products and noodles (Japanese) by gas-liquid chromatography with electron-capture detection. J Agric Food Chem 38:2154–2159
3. Lu CP, Lin CT, Chang CM et al (2011) Nitrophenylboronic acids as highly chemoselective probes to detect hydrogen peroxide in foods and agricultural products. J Agric Food Chem 59:11403–11406
4. Wu P, Qian Y, Du P et al (2012) Facile synthesis of nitrogen-doped graphene for measuring the releasing process of hydrogen peroxide from living cells. J Mater Chem 22:6402–6412
5. Bartlett PN, Birkin PR, Wang JH et al (1998) An enzyme switch employing direct electrochemical communication between horseradish peroxidase and a poly(aniline) film. Anal Chem 70:3685–3694
6. Wang Y, Shao Y, Matson DW et al (2010) Nitrogen-doped graphene and its application in electrochemical biosensing. ACS Nano 4:1790–1798
7. Shan C, Yang H, Song J et al (2009) Direct electrochemistry of glucose oxidase and biosensing for glucose based on graphene. Anal Chem 81:2378–2382
8. Hurdis EC, Romeyn H (1954) Accuracy of determination of hydrogen peroxide by cerate oxidimetry. Anal Chem 26:320–325
9. Klassen NV, Marchington D, McGowan HCE (1994) H_2O_2 determination by the I_3^- method and by $KMnO_4$ titration. Anal Chem 66:2921–2925
10. Chang MCY, Pralle A, Isacoff EY et al (2004) A selective, cell-permeable optical probe for hydrogen peroxide in living cells. J Am Chem Soc 126:15392–15393
11. King DW, Cooper WJ, Rusak SA et al (2007) Flow injection analysis of H2O2 in natural waters using acridinium ester chemiluminescence: method development and optimization using a kinetic model. Anal Chem 79:4169–4176
12. Jia J, Wang B, Wu A et al (2002) A method to construct a third-generation horseradish peroxidase biosensor: self-assembling gold nanoparticles to three-dimensional sol–gel network. Anal Chem 74:2217–2223
13. Luo XL, Xu JJ, Zhang Q et al (2005) Electrochemically deposited chitosan hydrogel for horseradish peroxidase immobilization through gold nanoparticles self-assembly. Biosens Bioelectron 21:190–196
14. Wang B, Zhang JJ, Pan ZY et al (2009) A novel hydrogen peroxide sensor based on the direct electron transfer of horseradish peroxidase immobilized on silica–hydroxyapatite hybrid film. Biosens Bioelectron 24:1141–1145
15. Wang L, Wang E (2004) A novel hydrogen peroxide sensor based on horseradish peroxidase immobilized on colloidal Au modified ITO electrode. Electrochem Commun 6:225–229
16. Cao Z, Jiang X, Xie Q et al (2008) A third-generation hydrogen peroxide biosensor based on horseradish peroxidase immobilized in a tetrathiafulvalene–tetracyanoquinodimethane/multiwalled carbon nanotubes film. Biosens Bioelectron 24:222–227
17. Zhang Y, Bo X, Luhana C et al (2013) Facile synthesis of a Cu-based MOF confined in macroporous carbon hybrid material with enhanced electrocatalytic ability. Chem Commun 49:6885–6887
18. Tian J, Liu Q, Ge C et al (2013) Ultrathin graphitic carbon nitride nanosheets: a low-cost, green, and highly efficient electrocatalyst toward the reduction of hydrogen peroxide and its glucose biosensing application. Nanoscale 5:8921–8924
19. Liu M, Liu R, Chen W (2013) Graphene wrapped Cu_2O nanocubes: non-enzymatic electrochemical sensors for the detection of glucose and hydrogen peroxide with enhanced stability. Biosens Bioelectron 45:206–212
20. Hao GP, Li WC, Qian D et al (2010) Rapid synthesis of nitrogen-doped porous carbon monolith for CO_2 capture. Adv Mater 22:853–857
21. Zhai Y, Dou Y, Zhao D et al (2011) Carbon materials for chemical capacitive energy storage. Adv Mater 23:4828–4850
22. Zhang J, Hu YS, Tessonnier JP et al (2008) CNFs@CNTs: superior carbon for electrochemical energy storage. Adv Mater 20:1450–1455
23. Lee JS, Park GS, Kim ST et al (2013) A highly efficient electrocatalyst for the oxygen reduction reaction: N-doped ketjenblack incorporated into Fe/Fe_3C-functionalized melamine foam. Angew Chem Int Ed 52:1026–1030
24. Jasinski R (1964) A new fuel cell cathode catalyst. Nature 201:1212–1213
25. Palaniselvam T, Biswal BP, Banerjee R (2013) Zeolitic imidazolate framework (ZIF)-derived, hollow-core, nitrogen-doped carbon nanostructures for oxygen-reduction reactions in PEFCs. Chem Eur J 19:9335–9342
26. Jiang Y, Lu Y, Lv X et al (2013) Enhanced catalytic performance of Pt-Free iron phthalocyanine by graphene support for efficient oxygen reduction reaction. ACS Catal 3:1263–1271
27. Parvez MK (2012) Nitrogen-doped graphene and its iron-based composite as efficient electrocatalysts for oxygen reduction reaction. ACS Nano 6:9541–9550
28. Sheng ZH, Shao L, Chen JJ et al (2011) Catalyst-free synthesis of nitrogen-doped graphene via thermal annealing graphite oxide with melamine and its excellent electrocatalysis. ACS Nano 5:4350–4358
29. Zhong H, Zhang H, Liu S et al (2013) Nitrogen-enriched carbon from melamine resins with superior oxygen reduction reaction activity. ChemSusChem 6:807–812
30. Stöhr B, Boehm HP, Schlögl R (1991) Enhancement of the catalytic activity of activated carbons in oxidation reactions by thermal treatment with ammonia or hydrogen cyanide and observation of a superoxide species as a possible intermediate. Carbon 29:707–720
31. Shin D, Jeong B, Mun BS et al (2013) On the origin of electrocatalytic oxygen reduction reaction on electrospun nitrogen-carbon species. J Phys Chem C 117:11619–11624
32. Xu X, Jiang S, Hu Z et al (2010) Nitrogen-doped carbon nanotubes: high electrocatalytic activity toward the oxidation of hydrogen peroxide and its application for biosensing. ACS Nano 4:4292–4298
33. Zhang L, Zhai Y, Gao N et al (2008) Sensing H_2O_2 with layer-by-layer assembled Fe_3O_4–PDDA nanocomposite film. Electrochem Commun 10:1524–1526

34. Zhang L, Fang Z, Ni Y et al (2009) Direct electrocatalytic oxidation of hydrogen peroxide based on nafion and microspheres MnO_2 modified glass carbon electrode. Int J Electrochem Sci 4:407–413
35. Bo X, Bai J, Wang L et al (2010) In situ growth of copper sulfide nanoparticles on ordered mesoporous carbon and their application as nonenzymatic amperometric sensor of hydrogen peroxide. Talanta 81:339–345
36. Ni P, Zhang Y, Sun Y et al (2013) Facile synthesis of Prussian blue@gold nanocomposite for nonenzymatic detection of hydrogen peroxide. RSC Adv 3:15987–15992
37. Chen XM, Cai ZX, Huang ZY et al (2013) Ultrafine palladium nanoparticles grown on graphene nanosheets for enhanced electrochemical sensing of hydrogen peroxide. Electrochim Acta 97:398–403
38. Maji SK, Dutta AK, Bhadu GR et al (2013) A novel amperometric biosensor for hydrogen peroxide and glucose based on cuprous sulfide nanoplates. J Mater Chem B 1:4127–4134
39. Guo CX, Sheng ZM, Shen YQ et al (2010) Thin-walled graphitic nanocages as a unique platform for amperometric glucose biosensor. ACS Appl Mater Interfaces 2:2481–2484
40. Ning R, Lu W, Zhang Y et al (2012) A novel strategy to synthesize Au nanoplates and their application for enzymeless H_2O_2 detection. Electrochim Acta 60:13–16
41. Miao YE, He S, Zhong Y et al (2013) A novel hydrogen peroxide sensor based on Ag/SnO_2 composite nanotubes by electrospinning. Electrochim Acta 99:117–123
42. Wang J, Gao H, Sun F et al (2013) Highly sensitive detection of hydrogen peroxide based on nanoporous Fe_2O_3/CoO composites. Biosens Bioelectron 42:550–555